Nonlinear dynamic waves in electromechanical excitable biological media

R. N. Miftakhov & M. W. Vannier
Department of Radiology, University of Iowa Hospitals and Clinics, USA

Abstract

A mathematical model of electromechanical conjugation in a longitudinal smooth muscle layer of the gut is formulated. The general assumptions of the model are based on electrophysiological and mechanical experimental data demonstrating slow oscillatory activity (at the resting state) and spiking activity (at the excited state) with concurrent development of active forces of contraction-relaxation. The myogenic syncytium is considered as a continuum of weakly connected oscillators. Strong connections among oscillators are provided by an intermittent fast propagating wave of depolarization along the syncytium. The description of electrical behavior of each oscillator is based on Hodgkin-Huxley formalism. Electromechanical coupling concludes intracellular calcium dependent mechanisms of force generation. Passive relaxation forces are mainly due to the elastic properties of the collagen and elastin fibers. The dynamics of the propagating nonlinear electromechanical wave of contraction-relaxation is studied numerically. The results demonstrate good qualitative and quantitative agreement with the results of physiological experiments.

1 Introduction

The gut can be considered as a continuum of spatially distributed weakly connected oscillators that are morphologically and functionally grouped into an infinite number of dynamically stable loci. The contractile components of a locus are presented by an outer (longitudinal) and an inner (circular) smooth muscle layers that are oriented in longitudinal and circular directions of the organ, respectively. Experimental data suggest that the longitudinal layer possesses anisotropic cable

and wave propagating properties, while the circular layer is isotropic. Each locus demonstrates a variety of patterns of electromechanical activity observed in vivo under normal physiological and pathological conditions. The medium can be adequately treated as homogeneous, in the normal state, while in pathological conditions there may be structural and functional inhomogeneities that can alter the dynamic demeanor of the system.

Modelling the biophysical processes governing behavior of the locus requires a system of smooth differential equations with several degrees of freedom for each oscillator. This includes the generation of an action potential due to activation-deactivation of ionic channels located on the cell membrane, an influx of calcium ions, and the initiation of a cascade of intracellular mechanisms of excitation-contraction coupling with the resultant production of the force of contraction-relaxation. Analyzing a two-dimensional excitable medium composed of oscillators is a difficult task because of the biological and mathematical complexity of a single oscillator per se and the constantly evolving nonlinear interrelations among linked oscillators. Nevertheless, with precise information on the electrophysiology and the biomechanics of smooth muscle we may formulate and accurately predict the dynamics of the generation and spread of nonlinear electromechanical waves in an anisotropic biological medium, i.e., the longitudinal muscle layer of the gut.

In this work, we consider a mathematical model of electromechanical conjugation in the longitudinal muscle layer of the gut, and study numerically the dynamics of the generation and propagation of the nonlinear electromechanical waves along it. This part of our investigation serves as the first step towards the formulation of a broad conceptual theory of gastrointestinal motility.

2 Formulation

2.1 Basic assumptions

The following working assumptions are made in model construction:

(i). The gut is a continuum of overlapping dynamically stable functional units. A functional unit is a structurally and geometrically defined part of the gut presented as a soft biological shell. It possesses the physiological (functional) properties of the entire gut.

(ii). Smooth muscle cells are spatially distributed autonomous oscillators connected homogeneously and weakly to form a myogenic syncytium. All oscillators can be divided into pools according to their natural frequencies (Ω_i) $(i = 1, L)$. If two oscillators have nearly equal frequency $(\Omega_i \sim \Omega_j)$ $(i, j = 1, L)$, then they weakly communicate; if $(\Omega_i = \Omega_j)$ $(i, j = 1, L)$, then they are strongly connected; if $(\Omega_i \neq \Omega_j)$ $(i, j = 1, N)$, then they are disconnected. Strong connections among pools are frequency modulated. Each oscillator is in a stable (silent) state. Transition to an excitable (firing) state occurs as a result of an external input.

(iii). Electrical slow waves (an intrinsic oscillatory phenomenon of the smooth muscle syncytium) have their own natural frequency.

(iv). Forces of contraction are a result of the activation of contractile proteins of the smooth muscle cells, which depends on the dynamics of intracellular calcium. Passive relaxation forces are predominantly due to the elastic properties of the connective tissue elements—the collagenous and elastin fibres. They are arranged in a planar network and provide structural support to the muscle cells.

(v). The mechanical activity of the myogenic medium is under the control of an external pacemaker cell located at the left boundary which generates the excitatory stimulus of given intensity and duration.

(The above assumptions are given more elaborate consideration in our previous publications [1]).

2.2 Mathematical model

The small intestinal segment dynamics:

$$
\begin{aligned}
\gamma_0 \left(\frac{\partial v_r}{\partial t} - \frac{v_s^2}{r} \right) = {} & \frac{\partial}{\partial \tilde{s}_1} \left[\left(k \frac{\partial (\lambda_c - 1)}{\partial t} + T^p (\lambda_c, \lambda_l) \right) e_{1r} \sqrt{g_{22}} \right] \\
& + \frac{\partial}{\partial \tilde{s}_2} \left[\left(k \frac{\partial (\lambda_l - 1)}{\partial t} + T^a (\lambda_l) + T^p (\lambda_c, \lambda_l) \right) e_{2r} \sqrt{g_{11}} \right] \\
& + p \sqrt{g}\, n_r, \\[4pt]
\gamma_0 \left(\frac{\partial v_s}{\partial t} + \frac{v_s v_r}{r} \right) = {} & \frac{\partial}{\partial \tilde{s}_1} \left[\left(k \frac{\partial (\lambda_c - 1)}{\partial t} + T^p (\lambda_c, \lambda_l) \right) e_{1s} \sqrt{g_{22}} \right] \\
& + \frac{\partial}{\partial \tilde{s}_2} \left[\left(k \frac{\partial (\lambda_l - 1)}{\partial t} + T^a (\lambda_l) + T^p (\lambda_c, \lambda_l) \right) e_{2s} \sqrt{g_{11}} \right] \\
& + p \sqrt{g}\, n_s, \\[4pt]
\gamma_0 \frac{\partial v_z}{\partial t} = {} & \frac{\partial}{\partial \tilde{s}_1} \left[\left(k \frac{\partial (\lambda_c - 1)}{\partial t} + T^p (\lambda_c, \lambda_l) \right) e_{1z} \sqrt{g_{22}} \right] \\
& + \frac{\partial}{\partial \tilde{s}_2} \left[\left(k \frac{\partial (\lambda_l - 1)}{\partial t} + T^a (\lambda_l) + T^p (\lambda_c, \lambda_l) \right) e_{2z} \sqrt{g_{11}} \right] \\
& + p \sqrt{g}\, n_z,
\end{aligned}
$$

$$ s \in (0, 2\pi r), \ z \in (0, 1), \ t > 0, \tag{1} $$

where the radial (v_r), circumferential (v_s) and longitudinal components (v_z) of the wall velocity vector are:

$$ v_r = \frac{dr}{dt}, \quad v_s = \frac{ds}{dt}, \quad v_z = \frac{dz}{dt}, \tag{2} $$

the rate of elongation (hereafter, the subscripts (l) and (c) are related to the longitudinal and circular muscle layers, respectively):

$$ \lambda_c = \frac{ds}{d\overset{\circ}{\tilde{s}}_1}, \qquad \lambda_l = \frac{dz}{d\overset{\circ}{\tilde{s}}_2}, \tag{3} $$

the components and determinant of the fundamental tensor are:

$$g_{ij} = \frac{\partial r}{\partial \tilde{s}_i} \frac{\partial r}{\partial \tilde{s}_j} + \frac{\partial s}{\partial \tilde{s}_i} \frac{\partial s}{\partial \tilde{s}_j} + \frac{\partial z}{\partial \tilde{s}_i} \frac{\partial z}{\partial \tilde{s}_j},$$

$$g = g_{11}g_{22} - g_{12}^2,$$

(4)

and the direction cosines of the outward normal, n_j, to the surface with respect to the cylindrical j-axis ($i = 1, 2; j = r, s, z$) are calculated as:

$$e_{ir} = \cos(\widehat{\tilde{s}_i, r}) = \frac{1}{\sqrt{g_{ii}}} \frac{\partial r}{\partial \tilde{s}_i}, \quad e_{is} = \frac{1}{\sqrt{g_{ii}}} \frac{\partial s}{\partial \tilde{s}_i}, \quad e_{iz} = \frac{1}{\sqrt{g_{ii}}} \frac{\partial z}{\partial \tilde{s}_i},$$

$$n_r = (e_{1s}e_{2z} - e_{1z}e_{2s}) \sqrt{g_{11}} \sqrt{g_{22}} / \sqrt{g},$$

$$n_s = (e_{1z}e_{2r} - e_{1r}e_{2z}) \sqrt{g_{11}} \sqrt{g_{22}} / \sqrt{g},$$

$$n_z = (e_{1r}e_{2s} - e_{1s}e_{2r}) \sqrt{g_{11}} \sqrt{g_{22}} / \sqrt{g}.$$

(5)

Here, the following notations are used: γ_0 — the linear density of a biomaterial in an undeformed state; T^p, T^a — the passive and active components, respectively, of the total force ($T_{c,l}$) of the wall; k — rheological parameter; p — intraluminal pressure; φ_l, φ_c — the electrical waves of depolarization of the longitudinal and circular muscle layers; $\tilde{s}_1$, $\tilde{s}_2$ — the Lagrangian coordinates of the bioshell.

The passive ($T^p_{(c,l)}$) components are calculated from:

$$T^p_{(c,l)} = \frac{\partial \gamma_0 W}{\partial (\lambda_{(c,l)} - 1)}.$$

(6)

Here, W = the strain energy density function of the connective tissue and passive muscular components:

$$\gamma_0 W = \frac{1}{2} \left[c_1 (\lambda_l - 1)^2 + 2c_3 (\lambda_l - 1)(\lambda_c - 1) + c_2 (\lambda_c - 1)^2 + \right.$$
$$\left. + c_{14} \exp \left(c_4 (\lambda_l - 1)^2 + c_5 (\lambda_c - 1)^2 + 2c_6 (\lambda_l - 1)(\lambda_c - 1) \right) \right].$$

(7)

For the active force ($T^a_{(l)}$) components, we assume:

$$T^a_{(l)} = \begin{cases} 0, & [\tilde{C}a^{2+}] \leq 0.1 \ \mu M, \\ c_7 + c_8[\tilde{C}a^{2+}]^4 + c_9[\tilde{C}a^{2+}]^3 + c_{10}[\tilde{C}a^{2+}]^2 + c_{11}[\tilde{C}a^{2+}], & 0.1 < [\tilde{C}a^{2+}] \leq 1 \ \mu M, \\ \max T^a, & [\tilde{C}a^{2+}] > 1 \ \mu M, \end{cases}$$

(8)

where: T^a — active force generated by smooth muscle syncytium; c_{1-11} — mechanical constants.

The characteristic feature of soft shells is the possibility of the simultaneous coexistence of unstressed, uniaxial and biaxial stress-strained zones. The creaseless shape occurs at: $\lambda_l > 1.0$; in a case of the development of creases, when $\lambda_l \leq 1.0$, the wrinkled area is modelled by a "smooth zone" made up by the

system of unbound filaments. This is determined by requirements which are geo-metrical relating to the conservation of smoothness of the surface of the bioshell, and force conditions relating to the continuity of membrane forces. Thus, for $T^p_{(c,l)}$ at the uniaxial stress-strained state of the bioshell, we assume:

$$T^p_{(c,l)} = \begin{cases} 0, & \lambda_{c,l} \leq 1.0, \\ c_{12}\left(\exp c_{13}\left(\lambda_{c,l} - 1\right) - 1\right), & \lambda_{c,l} > 1.0. \end{cases} \tag{9}$$

The dynamics of propagation of the electrical wave, φ_l, along the anisotropic longitudinal muscle layer is defined as:

$$C_m \frac{\partial \varphi_l}{\partial t} = I_{m1}\left(\tilde{s}_1, \tilde{s}_2\right) + I_{m2}\left(\tilde{s}_1 - \tilde{s}_1', \tilde{s}_2 - \tilde{s}_2'\right) - I^*_{\text{ionic}}, \tag{10}$$

where I_{m1}, I_{m2} are the transmembrane currents per unit volume:

$$I_{m1}\left(\tilde{s}_1, \tilde{s}_2\right) = M_{vs} \left\{ -\frac{2\left(\mu_{\tilde{s}_1} - \mu_{\tilde{s}_2}\right)}{\left(1 + \mu_{\tilde{s}_1}\right)\left(1 + \mu_{\tilde{s}_2}\right)} \operatorname{arctg}\left(\frac{d\tilde{s}_1}{d\tilde{s}_2}\sqrt{\frac{G_{\tilde{s}_2}}{G_{\tilde{s}_1}}}\right) + \right.$$

$$\left. + \frac{g^*_{0\tilde{s}_1}}{G_{\tilde{s}_1}} \right\} \left(\frac{\partial}{\partial \tilde{s}_1}\left(\frac{g^*_{0\tilde{s}_1}}{\lambda_c}\frac{\partial \varphi_l}{\partial \tilde{s}_1}\right) + \frac{\partial}{\partial \tilde{s}_2}\left(\frac{g^*_{0\tilde{s}_2}}{\lambda_l}\frac{\partial \varphi_l}{\partial \tilde{s}_2}\right)\right),$$

$$I_{m2}\left(\tilde{s}_1, \tilde{s}_2\right) = M_{vs} \iint_S \frac{\left(\mu_{\tilde{s}_1} - \mu_{\tilde{s}_2}\right)}{2\pi\left(1 + \mu_{\tilde{s}_1}\right)\left(1 + \mu_{\tilde{s}_2}\right)G} \times \tag{11}$$

$$\times \frac{\left(\tilde{s}_2 - \tilde{s}_2'\right)^2 / G_{\tilde{s}_2} - \left(\tilde{s}_1 - \tilde{s}_1'\right)^2 / G_{\tilde{s}_1}}{\left[\left(\tilde{s}_1 - \tilde{s}_1'\right)^2 / G_{\tilde{s}_1} + \left(\tilde{s}_2 - \tilde{s}_2'\right)^2 / G_{\tilde{s}_2}\right]^2} \times$$

$$\times \left(\frac{\partial}{\partial \tilde{s}_1}\left(\frac{g^*_{0\tilde{s}_1}}{\lambda_c}\frac{\partial \varphi_l}{\partial \tilde{s}_1}\right) + \frac{\partial}{\partial \tilde{s}_2}\left(\frac{g^*_{0\tilde{s}_2}}{\lambda_l}\frac{\partial \varphi_l}{\partial \tilde{s}_2}\right)\right) ds_1'\, ds_2'.$$

Here,

$$\mu_{\tilde{s}_1} = g^*_{0\tilde{s}_1}/g^*_{i\tilde{s}_1}, \qquad \mu_{\tilde{s}_2} = g^*_{0\tilde{s}_2}/g^*_{i\tilde{s}_2},$$

$$G_{\tilde{s}_1} = \frac{g^*_{0\tilde{s}_1} + g^*_{i\tilde{s}_1}}{\lambda_c}, \quad G_{\tilde{s}_2} = \frac{g^*_{0\tilde{s}_2} + g^*_{i\tilde{s}_2}}{\lambda_l}, \quad G = \sqrt{G_{\tilde{s}_1}G_{\tilde{s}_2}}, \tag{12}$$

and the following notations are accepted: C_m — the capacitance of smooth mus-cle; $g^*_{i\tilde{s}_1}, g^*_{i\tilde{s}_2}, g^*_{0\tilde{s}_1}, g^*_{0\tilde{s}_2}$ — the maximal intracellular (the subscript (i)) and inter-stitial space (the subscript (0)) conductivity of the longitudinal and circular muscle layers in the longitudinal and circumferential directions, respectively; M_{vs} — the membrane volume-to-surface ratio, I^*_{ionic} — the total ionic current:

$$I^*_{\text{ionic}} = \bar{g}_{\text{Na}} m^{*3} h^* \left(\varphi_{(l)} - \bar{\varphi}_{\text{Na}}\right) + \bar{g}_K n^{*4}\left(\varphi_{(l)} - \bar{\varphi}_K\right) + \bar{g}_\theta\left(\varphi_{(l)} - \bar{\varphi}_\theta\right). \tag{13}$$

Here, $\bar{g}_{\text{Na}}, \bar{g}_K, \bar{g}_\theta$ are the maximal conductances; m^*, h^*, and n^* are the probabilities of opening of the ion gates, and $\bar{\varphi}_{\text{Na}}, \bar{\varphi}_K, \bar{\varphi}_\theta$ are the reversal poten-tials of Na^+, K^+, and Cl^- currents, respectively, in smooth muscles.

The dynamics of change in the probability variables can be obtained from the solution of the first-order equation:

$$\frac{dy}{dt} = \alpha_y y - \beta_y (1 - y),\tag{14}$$

where y refers to m^*, h^*, and n^*, respectively. The activation, α_y^*, and deactivation, β_y^*, parameters for smooth muscle satisfy the following relations:

$$\begin{aligned}
\alpha_m^* &= \frac{0.005 \left(\varphi_{(l)} - \bar{\varphi}_m\right)}{\left(-1 + \exp 0.1 \left(\varphi_{(l)} - \bar{\varphi}_m\right)\right)}, \\
\beta_m^* &= 0.2 \exp \left(\left(\varphi_{(l)} + \bar{\varphi}_m\right)/38\right), \\
\alpha_h^* &= 0.014 \exp \left(-\left(\varphi_{(l)} + \bar{\varphi}_h\right)/20\right), \\
\beta_h^* &= 0.2/\left(1 + \exp 0.2 \left(\bar{\varphi}_h - \varphi_{(l)}\right)\right), \\
\alpha_n^* &= \frac{0.006 \left(\varphi_{(l)} - \bar{\varphi}_n\right)}{\left(-1 + \exp 0.1 \left(\varphi_{(l)} - \bar{\varphi}_n\right)\right)}, \\
\beta_n^* &= 0.75 \exp 0.1 \left(\bar{\varphi}_n - \varphi_{(l)}\right).
\end{aligned}\tag{15}$$

The myoelectrical activity in a locus of the small bowel is governed by the dynamics of voltage-dependent Ca^{2+} channels (L- and T-type), mixed Ca^{2+}–K^+ and K^+ channels and leak (chloride) channels. Thus the system of equations is a linear sum of the five ionic currents:

$$\alpha C_m \frac{d\varphi}{dt} = -(I_{Ca}^f + I_{Ca}^s + I_{Ca-K}^* + I_K^* + I_{Cl}^*).\tag{16}$$

Here, C_m is the membrane capacitance, φ is the membrane potential and $I_{(i)}$ are ionic currents carried by different ions and defined as: I_{Ca}^f, I_{Ca}^s — the fast and slow inward calcium currents via T- and L-type voltage-dependent Ca^{2+} channels, respectively:

$$\begin{aligned}
I_{Ca}^f &= \tilde{g}_{Ca}^f \tilde{m}_I^3 \tilde{h}(\varphi - \tilde{\varphi}_{Ca}^*), \\
I_{Ca}^s &= \tilde{g}_{Ca}^s \tilde{x}_{Ca}(\varphi - \tilde{\varphi}_{Ca}^*);
\end{aligned}\tag{17}$$

I_{Ca-K}^*, I_K^* — the outward calcium activated potassium and voltage-activated potassium currents, respectively:

$$\begin{aligned}
I_K^* &= \tilde{g}_K^* \tilde{n}^4 (\varphi - \tilde{\varphi}_K^*), \\
I_{Ca-K}^* &= \tilde{g}_{Ca-K}^* [\tilde{Ca}^{2+}](\varphi - \tilde{\varphi}_K^*)/(0.5 + [\tilde{Ca}^{2+}]);
\end{aligned}\tag{18}$$

and I_{Cl}^* — the leak chloride current:

$$I_{Cl}^* = \tilde{g}_{Cl}^*(\varphi - \tilde{\varphi}_{Cl}^*),\tag{19}$$

where: $\tilde{\varphi}_{Ca}^*$, $\tilde{\varphi}_K^*$, $\tilde{\varphi}_{Cl}^*$ are the reversal potentials for the respective currents; $[\tilde{Ca}^{2+}]$ is the intracellular concentration of calcium ions in the functional unit; $\tilde{g}_{Ca}^f$, $\tilde{g}_{Ca}^s$, $\tilde{g}_K^*$, $\tilde{g}_{Ca-K}^*$, $\tilde{g}_{Cl}^*$ are, respectively, the maximal conductances of voltage-dependent

Ca^{2+}, Ca^{2+}-activated K^+ channels and a leak Cl^- conductance; $\tilde{m}$, $\tilde{h}$, $\tilde{n}$ and $\tilde{x}_{Ca}$ are dynamic variables of these channels whose kinetics is described by:

$$\tilde{m}_I = \tilde{\alpha}_m / \left(\tilde{\alpha}_m + \tilde{\beta}_m \right),$$

$$\frac{d\tilde{h}}{dt} = \left(\tilde{\alpha}_h \left(1 - \tilde{h} \right) - \tilde{\beta}_h \tilde{h} \right) / \alpha\lambda,$$

$$\frac{d\tilde{n}}{dt} = \left(\tilde{\alpha}_n \left(1 - \tilde{n} \right) - \tilde{\beta}_n \tilde{n} \right) / \alpha\lambda, \tag{20}$$

$$\frac{d\tilde{x}_{Ca}}{dt} = (1 + (\exp 0.15(-\varphi - 50))^{-1} - \tilde{x}_{Ca}) / \alpha\tau_{x_{Ca}},$$

$$\frac{d[\tilde{Ca}^{2+}]}{dt} = \frac{\rho}{\alpha} (K_c \tilde{x}_{Ca} (\tilde{\varphi}_{Ca} - \varphi) - [\tilde{Ca}^{2+}]),$$

where:

$$\tilde{\alpha}_m = 0.1(50 - \tilde{\varphi})/(\exp(5 - 0.1\tilde{\varphi}) - 1),$$

$$\tilde{\beta}_m = 4\exp(25 - \tilde{\varphi})/18,$$

$$\tilde{\alpha}_h = 0.07\exp(25 - \tilde{\varphi})/20,$$

$$\tilde{\beta}_h = 1/(1 + \exp(5.5 - 0.1\tilde{\varphi})), \tag{21}$$

$$\tilde{\alpha}_n = 0.01(55 - \tilde{\varphi})/(\exp((55 - \tilde{\varphi})/10) - 1),$$

$$\tilde{\beta}_n = 0.125\exp(45 - \tilde{\varphi})/80;$$

here: $\tilde{\varphi} = (127\varphi + 8265)/105$; $\tau_{x_{Ca}}$ is the time constant and ρ, K_c are parameters referred to the dynamics of calcium channels; α is a constant; parameters $\tilde{\alpha}$ and $\tilde{\beta}$ have the same meaning as in above.

Therefore, the evolution of L-type voltage-dependent Ca^{2+}-channels is defined as:

$$\tilde{g}_{Ca}^s = \delta(\varphi_p^+)\tilde{g}_{Ca}^s; \tag{22}$$

here: $\delta(\varphi_p^+)$ is the function defined as: $\delta(\varphi_p^+) = 1$ when $\varphi_p^+ \geq \varphi_p^*$ (φ_p^* — threshold value) and $\delta(\varphi_p^+) = 0$ otherwise.

The initial conditions assume that the system is in the resting state.

Boundary conditions. The intestinal segment undergoes isometric contractions:

$$\forall t > 0: \text{ at } z = 0, 1: v_s = v_r = v_z = 0. \tag{23}$$

The discharge of the pacemaker causes the development of the wave of depolarization in the longitudinal smooth muscle. The left boundary of the intestinal segment remains in the resting state throughout:

$$\forall t > 0: \ \varphi_{(c,l)}\big|_{\tilde{s}_1, \tilde{s}_2 = 1} = 0.$$

The system (1), (11) and (16) was solved numerically.

3 Results

In the unexcited state, the oscillatory slow waves of equal frequency are recorded at any one point on the syncytium. The average amplitude of the waves is 22.5 mV and the frequency is 0.44 Hz. The observed corresponding oscillations of intracellular calcium are out of phase with the membrane potential. The velocity of influx of Ca^{2+} is 0.06 μM/s and the maximum concentration of internal Ca^{2+} reached is 0.46 μM. The rise in free intracellular calcium leads to activation of the contractile protein system with the generation of the force of contraction (T^a). It is concomitant in phase and time with changes in $[Ca^{2+}]$ and undulates at an average amplitude 4.8 g.

The discharge of a pacemaker cell located on the left boundary of the syncytium produces a wave of depolarization φ_l (Fig. 1). The amplitude of the wave is 69–72 mV and the length is 0.5–0.55 cm. With the achievement of the threshold level of depolarization ($\varphi_l \geq 30$ mV), there is a subsequent increase in permeability of the L-type Ca^{2+} channels on the smooth muscle membrane. This causes a rapid influx of extracellular Ca^{2+} into the cell. A rise in the concentration of free intracellular Ca^{2+} transforms the oscillator from its slow oscillatory mode to an excitatory state with the generation of high amplitude action potentials. The latter occur predominantly on the crests of slow waves. The pattern of spiking changes from bursting chaos with variable frequency to a regular busting mode at which time the maximum $\nu = 21$ Hz is observed. The amplitude of the action potentials is small at the beginning, $\varphi = 23$ mV, and reaches its maximum, $\varphi = 72$ mV, with full excitation of the system. As a result of the above changes, both the concentration of free available internal Ca^{2+} ions and the intensity of the active force increase.

The dynamics of the activation of the spatially distributed oscillators follows the front of the wave φ_l. The time delay of the inducement of action potentials corresponds to the intensity of the propagation of φ_l. Thus, Δt between the beginning of the recording of action potentials at two points is 1.4 s. It reduces to zero as the front φ_l straightens and the velocity of the propagation reaches its maximum value $\simeq 2.5$ cm/s. There is a corresponding delay in the generation of the active force of contraction.

A brief and small wave of relaxation, T^p, always precedes the propagating wave of contraction (not shown). It is due to stretching of the elastic collagen and elastin fibers of the medium. The distribution of T^p along the syncytium is uniform with max $T^p = 3.2$ g/cm. The dynamics of T^a recorded at each oscillator differs from the space distributed wave of contraction over the syncytium. Thus, the maximum force generated by a cluster of cells within an oscillator is 14.4 g and its variation in time is conjoint in phase with oscillations of internal Ca^{2+}. The redistribution of force among the adjacent oscillators within the myogenic medium results in smoothing of the mechanical wave T^a along the computational domain. The wave T^a expands at a velocity $\simeq 1.9$–2.0 cm/s from the point of origin on the left boundary. Its anterior front has the form of an ellipse at the beginning of the
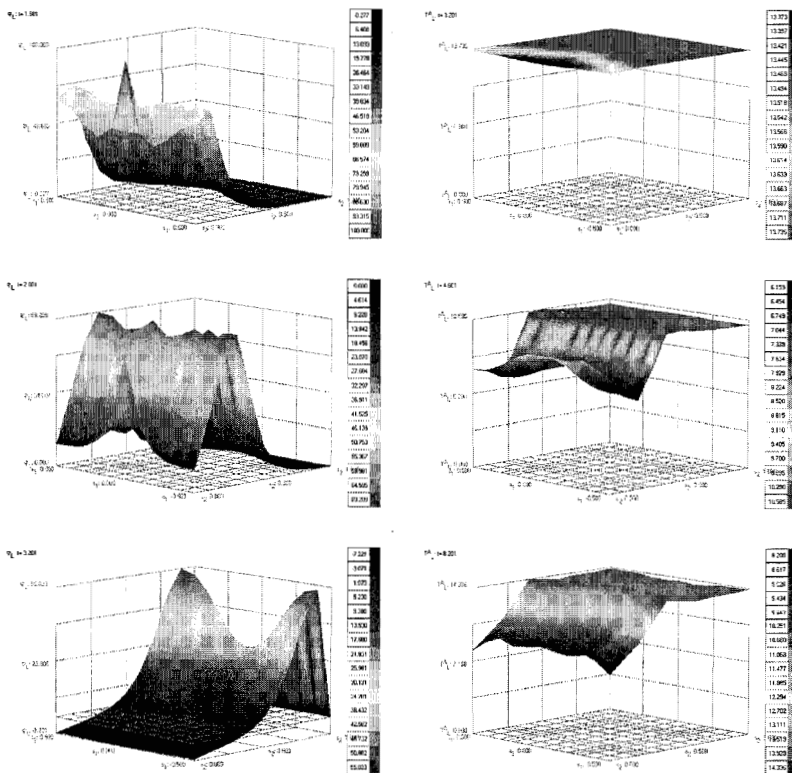
FIGURE 1. Distribution of the electrical wave (left column) and active force (right column) in the longitudinal smooth muscle layer of the gut at different moments in the dynamic process presented on a cylindrical envelope.

process. It straightens with diffuse excitation of the medium and causes a uniform contraction of the medium (Fig. 1).

The dynamics of the propagation of the nonlinear electromechanical waves differs from that described above under simulated pathological conditions (altered permeability of ionic channels, application of pharmacological compounds, changes in the stiffness of the connective tissue elements, etc.). For example, the addition of tetrodotoxin (TTX), a sodium channel antagonist, to the system abolishes the spread of the wave of depolarization φ_l. However, it does not affect oscillatory activity of the smooth muscle pools. They continue to generate non-propagating slow waves at their intrinsic frequencies with the concomitant production of active forces. On the other hand, the application of calciseptine, a specific L-type Ca^{2+} channel antagonist, abolishes slow wave activity while the dynamics of the wave φ_l remains unaltered.

4 Concluding remarks

Due to the absence of a theoretical framework, intestinal motility long seemed an empirically realized process, largely incomprehensible and unpredictable. We have accumulated new insight into the gastrointestinal tract per se from the application of the reductionist strategies of modern biology. The resultant data, however, describe a vast array of nonlinear processes whose interactions remain inexplicable. The situation is aggravated by sometimes inaccurate and misleading interpretation of experimental results. For example, the notion of the propagating slow waves that play a crucial role in the coordination of peristaltic activity was borrowed from the physics of waves and incorrectly adapted to a description of the oscillatory processes occurring in the muscle layers. This is but one example where false assumptions regarding bowel motility can lead to misunderstanding the true physiology of this complex dynamic organ.

We have begun to integrate structural elements of a multicomponent system (the gut) into a conceptual model that will provide a foundation for the theory of gastrointestinal motility. The model described above considers a soft biological shell formed by the longitudinal smooth muscle layer. Its ability to generate slow waves and high amplitude spikes have been studied extensively in previous publications [2–4]. The simulation of the spatial distributed oscillatory pools allowed us to reproduce adequately the dynamics of the electromechanical wave. It is clear from the simulations that the wave of depolarization is required to strongly connect separate pools for a coordinated contraction-relaxation of the myogenic syncytium. The model explains a puzzling observation related to the effect of TTX on the myoelectrical activity of the gut. The application of TTX does not abolish the production of slow waves but inhibits the contraction of muscle. It is obvious from the above considerations that sodium channels have no effect on the oscillatory activity. However, their blockade hinders the generation of the wave of depolarization and, as a result, no contractions are recorded.

References

[1] Miftakhov, R. & Abdusheva, G.R., Numerical simulation of excitation-contraction coupling in a locus of the small bowel, *Biological Cybernetics*, **74(5)**, pp. 455–467, 1996.

[2] Miftakhov, R., Abdusheva, G.R. & Wingate, D.L., Model Predictions of myoelectrical activity of the small bowel, *Biological Cybernetics*, **74(2)**, pp. 167–179, 1996.

[3] Miftakhov, R., Abdusheva, G.R. & Christensen, J., Numerical simulation of motility patterns of the small bowel, 1: Formulation of a mathematical model, *Journal of Theoretical Biology*, **197**, pp. 89–112, 1999.

[4] Miftakhov, R., Abdusheva, G.R. & Christensen J., Numerical simulation of motility patterns of the small bowel, 2: Comparative pharmacological validation of a model, *Journal of Theoretical Biology*, **200**, pp. 261–290, 2000.